

# Electronic Polarization Control Algorithms for Coherent Optical Transmission

Reinhold Noé, *Senior Member, IEEE*, Timo Pfau, *Member, IEEE*, Mohamed El-Darawy, *Student Member, IEEE*, and Sebastian Hoffmann, *Member, IEEE*

**Abstract**—In this paper, we review the nondata-aided constant-modulus algorithm (CMA) and a data-aided decision-directed algorithm (DDA) for polarization control and propose different extensions to both algorithms to improve their performance. The first extension to the CMA enables a common carrier recovery (CCR) through differential phase compensation (DPC-CMA). The second extension adapts the CMA for quadrature amplitude modulation signals (CMA-QAM). Both extensions can be combined to form a DPC-CMA for QAM signals (DPC-CMA-QAM). A new, modified DDA (MDDA) considerably increases polarization tracking speeds compared to the original DDA (ODDA). It is also usable for QAM signals. The algorithms are compared in simulations of QPSK and 16-QAM transmission systems. The results show that the DPC extension for the CMA in combination with CCR doubles laser linewidth tolerance and also the CMA-QAM triples polarization control speed compared to the standard CMA for QAM signals. The MDDA is  $\sim 1.6$ – $4$  times faster than the CMA variants and is, at least when QAM signals are transmitted, more hardware-efficient.

**Index Terms**—Coherent detection, digital signal processing, optical fiber communication, polarization.

## I. INTRODUCTION

COHERENT digital receivers for polarization-multiplexed QPSK are a main contender for future 100 GbE transmission. This paper deals with one key part of these: electronic polarization control. High control speed, low complexity, phase noise, and modulation format tolerance are desirable and shall be discussed. New, more powerful algorithms will be presented in this context.

The phase noise tolerance of a polarization-multiplexed receiver can be improved by a common carrier recovery (CCR) for both polarizations [1], [2]. But this is possible only if the preceding polarization control compensates for the possible phase offset between the two polarizations. While this functionality is inherent in decision-directed polarization controllers, nondata-aided (NDA) algorithms, like the standard constant-modulus algorithm (CMA), do not compensate for this offset [3], [4].

Manuscript received September 1, 2009; revised September 13, 2009 and November 6, 2009; accepted November 6, 2009. Date of publication February 18, 2010; date of current version October 6, 2010.

R. Noé, M. El-Darawy, and S. Hoffmann are with the University of Paderborn, Optical Communication and High-Frequency Engineering, 33098 Paderborn, Germany (e-mail: noe@upb.de; eldarawy@ont.upb.de; hoffmann@ont.upb.de).

T. Pfau was with the University of Paderborn, Electrical Engineering and Information Technology, Optical Communication and High-Frequency Engineering, 33098 Paderborn, Germany. He is now with Bell Laboratories, Alcatel-Lucent, Murray Hill, NJ 07974 USA (e-mail: pfau@ont.upb.de).

Color versions of one or more of the figures in this paper are available online at <http://ieeexplore.ieee.org>.

Digital Object Identifier 10.1109/JSTQE.2009.2039920

In Section II, we review the standard CMA and then present an extended version, i.e., differential phase compensation CMA (DPC-CMA), which additionally compensates the phase difference between the two polarization channels to allow for a CCR [5].

If the transmission distance is not extreme, 16-quadrature amplitude modulation (QAM) is more rewarding than QPSK because it doubles spectral efficiency or even channel bit rate. A phase-noise-tolerant carrier recovery algorithm for QAM signals has been published recently [6]. In Section III, we, therefore, extend standard CMA and DPC-CMA for QAM signals also [7]. This allows the implementation of phase-noise-tolerant QAM receivers, because one CCR may be used, with fast polarization control. Important earlier works in this field include a CMA for 8-QAM signals [8] and a decision-directed CMA for QAM [9]. Our CMA-QAM variant is closely related to the radiant directed algorithm [10].

Another class of algorithms is data-aided. This class includes the original decision-directed algorithm (ODDA) for electronic polarization control that was presented in [1] and tested at up to 40 krad/s polarization tracking speed [11]. In Section III, we review the ODDA and then present a modified DDA (MDDA).

Section IV starts with Monte Carlo simulations of a QPSK system. The differentially phase-compensated CMA (DPC-CMA) is compared with the standard CMA [4]. ODDA and MDDA are compared with the CMA. The penalty as a function of control gain is calculated for all four algorithms.

While ODDA and MDDA also work straightforward for 16-QAM, this needs to be proved for the CMA-QAM variant. The DPC feature proves superior because in a 16-QAM system, a CCR is needed to increase linewidth tolerance and minimize hardware effort.

In Section V, the hardware efforts for implementation of the various algorithms are briefly compared. Due to the superior performance and low complexity, we recommend the MDDA, especially for QAM transmission.

Section VI concludes this paper.

## II. CONSTANT-MODULUS ALGORITHM AND ITS EXTENSIONS

### A. Standard Constant-Modulus Algorithm

The standard CMA works as follows (see Fig. 1): let

$$\mathbf{c} = \begin{bmatrix} c_1 \\ c_2 \end{bmatrix} \quad (1)$$

be the transmitted complex signal (Jones) vector. The fiber Jones matrix  $\mathbf{J}$  is invertible, and therefore, has only a finite

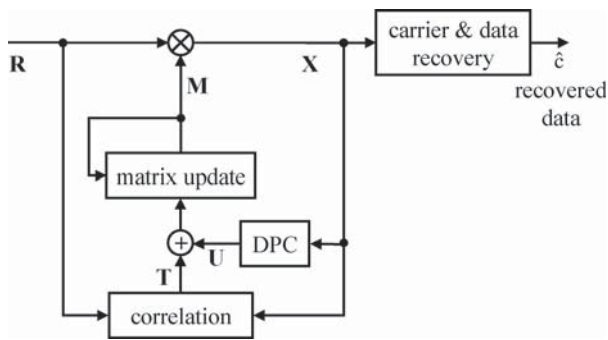


Fig. 1. Block diagram of CMA, including its extensions for DPC and QAM (not visible).

polarization-dependent loss. Now

$$\mathbf{R} = \begin{bmatrix} R_1 \\ R_2 \end{bmatrix} = e^{j\varphi_{IF}} \mathbf{J}\mathbf{c} \quad (2)$$

is the complex signal (Jones) vector in a coherent polarization diversity receiver, where  $\varphi_{IF}$  is the phase difference between the transmitter and local oscillator lasers. Let  $\mathbf{M}$  be the electronic polarization control matrix; then

$$\mathbf{X} = \begin{bmatrix} X_1 \\ X_2 \end{bmatrix} = \mathbf{M}\mathbf{R} = e^{j\varphi_{IF}} \mathbf{M}\mathbf{J}\mathbf{c} \quad (3)$$

is the corrected signal vector, ready for carrier and data recovery. The signals are sampled at the symbol rate, and a perfect clock recovery is assumed. The error signal matrix is defined and determined as

$$\mathbf{T} = \begin{bmatrix} 1 - |X_1|^2 & 0 \\ 0 & 1 - |X_2|^2 \end{bmatrix} \mathbf{X}\mathbf{R}^+ \quad (4)$$

in an NDA approach. The + sign means Hermitian conjugation. In the standard CMA [3],  $\mathbf{M}$  is incrementally updated as

$$\mathbf{M} := \mathbf{M} + g\mathbf{T} \quad (0 < g \ll 1). \quad (5)$$

This algorithm will generally make the error signal matrix  $\mathbf{T}$  vanish. This is achieved as soon as the conditions  $|X_1| = 1$  and  $|X_2| = 1$  are fulfilled. In this process, no phase condition is imposed on  $X_1$  and  $X_2$ . Therefore,  $\mathbf{M}\mathbf{J}$  need not be the unity matrix, but can more generally be

$$\mathbf{M}\mathbf{J} = \begin{bmatrix} e^{j\varphi_1} & 0 \\ 0 & e^{j\varphi_2} \end{bmatrix} \quad (6)$$

because this results in a corrected signal vector

$$\mathbf{X} = \begin{bmatrix} e^{j(\varphi_1 + \varphi_{IF})} c_1 \\ e^{j(\varphi_2 + \varphi_{IF})} c_2 \end{bmatrix} \quad (7)$$

with arbitrary phases. The angles  $\varphi_p$  of the polarizations  $p = 1, 2$  are recovered together with  $\varphi_{IF}$  in separate carrier recoveries (SCRs), one for each polarization. This is uneconomical. If there is a lot of phase noise, as in QAM transmission, SCRs may even fail to work.

It is worth noting that a mixture between SCRs and CCRs is advantageous for nonlinear transmission [12].

### B. Differentially Phase-Compensated Constant-Modulus Algorithm

We extended the CMA to compensate the phase difference  $\varphi_1 - \varphi_2$ , and, of course, modulo  $2\pi/q$ , where  $q$  is the number of ambiguous phase states. For QPSK and normal QAM,  $q = 4$  holds. This enables the use of one carrier for demodulation of both polarizations, which is generated in a CCR. In this DPC-CMA,  $\mathbf{M}$  is updated according to (3) and (4), and

$$\mathbf{M} := \mathbf{M} + g(\mathbf{T} + \mathbf{U}) \quad (8)$$

$$\mathbf{U} = \begin{bmatrix} -j & 0 \\ 0 & j \end{bmatrix} \mathbf{M} \frac{1}{2} \Delta\varphi \quad (9)$$

$$\Delta\varphi = (\arg X_1 - \arg X_2) = (\varphi_1 - \varphi_2) \quad (10)$$

with the definition

$$\alpha] = ((\alpha + \pi/q) \bmod (2\pi/q)) - \pi/q \quad (11)$$

Thus,  $\Delta\varphi$  is an angle given modulo  $2\pi/q$  ( $=\pi/2$  for QPSK) in the interval  $[-\pi/q, \pi/q]$  ( $=[-\pi/4, \pi/4]$  for QPSK). The left-hand side of (8) is the new, updated polarization control matrix. On the right-hand side, old, available quantities are used for its calculation.

For a perturbation  $\Delta\varphi$  alone (i.e.,  $\mathbf{T} = \mathbf{0}$ ), (8) and (9) mean that in the modified  $\mathbf{M}$ , the first and the second line will be multiplied by  $1 \mp jg\Delta\varphi/2 \approx e^{\mp jg\Delta\varphi/2}$ , thereby diminishing the unwanted differential phase shift.

### C. Constant-Modulus Algorithm Extended for Quadrature Amplitude Modulation (CMA-QAM, DPC-CMA-QAM)

If this standard CMA is applied to  $M$ -ary QAM signals, then the control gain  $g$  has to be chosen very small. This is because QAM signals assume different powers, and not unit powers like QPSK. Therefore, the terms  $1 - |X_p|^2$  in (4) become extremely noisy. We solve this problem by what we call CMA-QAM: (4) is modified to become

$$\mathbf{T} = \begin{bmatrix} \Delta P_{1,\min} & 0 \\ 0 & \Delta P_{2,\min} \end{bmatrix} \mathbf{X}\mathbf{R}^+ \quad (12)$$

$$\Delta P_{p,\min} = [\Delta P_{p,h_p}]_{\min_{h_p}} |\Delta P_{p,h_p}| \quad (13)$$

$$\Delta P_{p,h_p} = \hat{P}_{p,h_p} - |X_p|^2. \quad (14)$$

Index  $p = 1, 2$  always stands for the two polarizations.  $h_p = 1, 2, \dots, H$  is the index of the power of a distortion-free signal in the respective polarization.  $\Delta P_{p,h_p}$  is the power difference between all  $H$  possible expected values  $\hat{P}_{p,h_p}$  of signal powers in case of zero-polarization crosstalk and the observed signal powers  $|X_p|^2$  in both polarizations:  $p = 1, 2$ .  $\Delta P_{p,\min}$  is the value of  $\Delta P_{p,h_p}$  among all power indexes  $h_p$  of a polarization that has the smallest magnitude, and hence, the most likely power difference. Once the algorithm has converged, all power

differences  $\Delta P_{p,\min}$  would be zero in the absence of noise. The number  $H$  of distortion-free signal powers  $\hat{P}_{p,h_p}$  equals the number of circles around the origin that are needed to touch all symbols in the chosen QAM constellation. The value is  $H = 1, 3, 6, 9$  for QPSK, 16-, 64-, and 256-QAM, respectively.

Now, we add the DPC feature to the CMA-QAM: a number of test phases

$$0 \leq \varphi_c < 2\pi/q \quad (15)$$

is subtracted from the observed phase difference (10). The test phases needed depend on the values of  $h_p$  that have been estimated in the minimization process [see (13)]. Depending on the estimated powers  $\hat{P}_{1,h_1}$  and  $\hat{P}_{2,h_2}$ , there are different numbers of test phases.

Then, one selects the following to be used in (9):

$$\Delta\varphi = [\Delta\varphi_c]_{\min|\Delta\varphi_c|} \quad (16)$$

$$\Delta\varphi_c = (\arg X_1 - \arg X_2 - \varphi_c + \varphi_f). \quad (17)$$

The various phase differences  $\Delta\varphi_c$  are found for the applicable set of test phases  $\varphi_c$  and are mapped modulo  $2(\pi/q)$  into the interval  $[-\pi/q, \pi/q]$ . Angle  $\Delta\varphi$  is the value of  $\Delta\varphi_c$  that has the lowest magnitude  $|\Delta\varphi_c|$ . For the time being, let  $\varphi_f = 0$ . If there is no noise and the differential phase shift is already compensated, then, ideally,  $\Delta\varphi$  becomes zero. In order to improve accuracy in the presence of noise, the phase difference can be weighted according to the available or estimated powers, for example, by using

$$\Delta\varphi = [\Delta\varphi_c]_{\min|\Delta\varphi_c|} \hat{P}_{1,h_1} \hat{P}_{2,h_2}. \quad (18)$$

Consider 16-QAM (with  $q = 4$ ) as an example. If each quadrature can assume the values  $-3, -1, 1, \text{ and } 3$ , then the combined power, defined as the squared magnitude, is one of 2, 10, and 18. We assume normalization with respect to the mean power 10. This brings the expected powers in the individual polarization channels to

$$\hat{P}_{p,h_p} = 0.2, 1, 1.8 \text{ for } h_p = 1, 2, 3. \quad (19)$$

The needed test phases are

$$\varphi_c = \begin{cases} 0, & \text{for } h_1, h_2 \in \{1, 3\} \\ 0, \pm 0.64, & \text{for } h_1 = h_2 = 2 \\ \pm 0.46, & \text{otherwise} \end{cases}. \quad (20)$$

The value 0.46 rad is the phase angle between the numbers  $(3 + j)$  and  $(1 + j)$ , which are proportional to QPSK symbols. The value 0.64 rad is the one between the numbers  $(3 + j)$  and  $(3 - j)$ . By taking modulo  $\pi/2$ , the value 0.64 is identical to  $-2 \times 0.46$ . The best suitable among the possible test phases  $\varphi_c$  is subtracted from the observed value,  $\arg X_1 - \arg X_2$ .

The CMA with DPC can, in this configuration, track a once-acquired optimum. However, we have observed occasional false initial locking. But only one locking point yields a product  $\mathbf{M}\mathbf{J}$  proportional to the unity matrix, while at other possible locking points, there is a static phase shift between the two polarization channels. In order to quit a false optimum, one can calculate  $\Delta\varphi$

[see (16)] not only for  $\varphi_f = 0$  but also for  $F$  equidistant phase offsets

$$\varphi_f = (f/F)(2\pi/q), \quad f \in \{0, 1, \dots, F-1\}. \quad (21)$$

A good choice is  $F = 8\sqrt{M}$ , i.e.,  $F = 32$  for 16-QAM. The squares of the various  $\Delta\varphi = \Delta\varphi(f, k)$  are added up over  $K$  subsequent symbols

$$W_f = \sum_{k=1}^K (\Delta\varphi(f, k))^2. \quad (22)$$

One determines the integer  $f$  that corresponds to the smallest  $W_f$ . This value of  $f$  indicates that a better optimum is available if one introduces a differential phase shift  $\varphi_f$  between the polarizations. Thus, after  $K$  symbols, one sets

$$\mathbf{M} := \begin{bmatrix} e^{j\varphi_f/2} & 0 \\ 0 & e^{-j\varphi_f/2} \end{bmatrix} \mathbf{M}. \quad (23)$$

Thereafter, the summation process (22) may start anew. But this is usually not needed because a single application of (23) generally yields a differential phase very close to the optimum, which is subsequently improved and tracked. As a consequence, the full set (17), (21) for all  $f$ , and (23) may be executed far less frequently than the tracking calculation for  $\varphi_f = 0$ . This reduces hardware effort.

A simpler way to avoid false locking is the following: behind the decision circuits, a framing information is detected, which indicates whether data are being received correctly in both polarization channels. If not, then (23) is executed with a suitably chosen  $\varphi_f$ , or with all values given in (21), until data recovery is correct. This does not slow down normal polarization control, since it occurs only at initial signal acquisition.

### III. DECISION-DIRECTED ALGORITHMS: ORIGINAL (ODDA) AND MODIFIED (MDDA)

#### A. Original Decision-Directed Algorithm

In the original decision-directed polarization control algorithm [1], the recovered symbol

$$\hat{\mathbf{c}} = \begin{bmatrix} \hat{c}_1 \\ \hat{c}_2 \end{bmatrix} \quad (24)$$

is correlated with the output signal of the polarization demultiplexer. The correlation matrix  $\mathbf{Q}$  is given by

$$\mathbf{Q} = \mathbf{X} e^{-j\hat{\varphi}} \hat{\mathbf{c}}^+. \quad (25)$$

where  $\hat{\varphi}$  is the estimated carrier phase. It is made available by the carrier recovery. The expectation  $\langle \mathbf{Q} \rangle$  of the matrix  $\mathbf{Q}$  is a perfect estimate of the matrix product  $\mathbf{M}\mathbf{J}$ . Therefore, by calculating and assigning

$$\mathbf{M} := \langle \mathbf{Q} \rangle^{-1} \mathbf{M} = \mathbf{J}^{-1} \mathbf{M}^{-1} \mathbf{M} = \mathbf{J}^{-1} \quad (26)$$

the polarization can be controlled penalty-free. Fig. 2 visualizes the structure of the algorithm.

The literal implementation of (26) in hardware poses a huge challenge, because the calculation of the inverse of a matrix

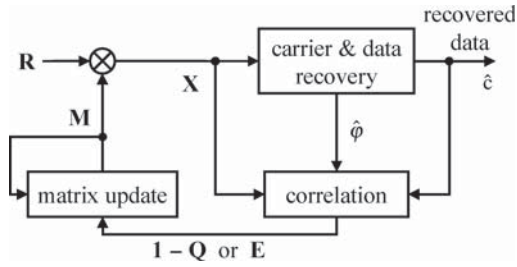


Fig. 2. Original (ODDA, using  $\mathbf{1} - \mathbf{Q}$ ) or modified (MDDA, using  $\mathbf{E}$ ) decision-directed algorithm for polarization control.

in a digital circuit is very complex. But the calculation can be simplified, using the Taylor series

$$\mathbf{Q}^{-1} = \sum_{i=0}^{\infty} (-1)^i (\mathbf{Q} - \mathbf{1})^i. \quad (27)$$

If  $\mathbf{Q}$  approaches the unity matrix  $\mathbf{1}$ , which is the goal of the polarization control, the Taylor series is dominated by its first-order element and the calculation of  $\mathbf{M}$  reduces to

$$\mathbf{M} := (\mathbf{1} + \mathbf{1} - \langle \mathbf{Q} \rangle) \mathbf{M} = \mathbf{M} + (\mathbf{1} - \langle \mathbf{Q} \rangle) \mathbf{M}. \quad (28)$$

In general, as  $\langle \mathbf{Q} \rangle \neq \mathbf{Q}$  applies, either several correlation results must be averaged to determine  $\langle \mathbf{Q} \rangle$  or  $\mathbf{M}$  must be updated incrementally with small control gain ( $0 < g \ll 1$ )

$$\mathbf{M} := \mathbf{M} + g(\mathbf{1} - \mathbf{Q}) \mathbf{M}. \quad (29)$$

This equation describes the update of the polarization control matrix coefficients, with  $\mathbf{Q}$ ,  $\mathbf{X}$ , and  $\hat{\mathbf{c}}$  given by (25), (3), and (24), respectively. For convenience, both possibilities can be combined in practice.

### B. Modified Decision-Directed Algorithm

Now, consider the case  $\mathbf{M}\mathbf{J} = \mathbf{1}$  and neglect noise and bit errors. Then, the equation  $|X_{1,2}|^2 = 1$  holds, and (4) yields a vanishing correction matrix  $\mathbf{T} = \mathbf{0}$ . Matrix  $\mathbf{M}$  is, therefore, left unchanged, as it should be. In contrast, the ODDA has the following weakness: on average, it achieves a vanishing average  $\langle \mathbf{1} - \mathbf{Q} \rangle = \mathbf{0}$ .  $\mathbf{M}\mathbf{J}$  becomes proportional to the unity matrix and there are no decision errors (in the absence of noise). The corrected signal vector is, with exception of the phase rotation to be undone in the carrier recovery, already identical with the recovered symbol input  $\hat{\mathbf{c}}$ . It holds that  $\hat{\mathbf{c}} = \mathbf{X}e^{-j\hat{\varphi}}$ . For QPSK, the elements of  $\hat{\mathbf{c}}$  are  $\hat{c}_{1,2} = (\pm 1 \pm j)/\sqrt{2}$ . According to (25), the momentary correlation matrices  $\mathbf{Q}$ , therefore, assume the following values:

$$\mathbf{Q} = \hat{\mathbf{c}}\hat{\mathbf{c}}^+ = \begin{bmatrix} 1 & j^{-m} \\ j^m & 1 \end{bmatrix} \quad (30)$$

where  $m$  is an integer that specifies by how many quadrants the QPSK symbols are separated in the complex plane. This means that the term  $\mathbf{1} - \mathbf{Q}$  is very disturbed by data; only the average  $\langle \mathbf{1} - \mathbf{Q} \rangle$  vanishes. The same problem also exists for other formats such as 16-QAM.

Therefore, it is better to replace  $\mathbf{1} - \mathbf{Q}$  by an error matrix

$$\mathbf{E} = \hat{\mathbf{c}}\hat{\mathbf{c}}^+ - \mathbf{X}e^{-j\hat{\varphi}}\hat{\mathbf{c}}^+ = (\hat{\mathbf{c}} - \mathbf{X}e^{-j\hat{\varphi}})\hat{\mathbf{c}}^+. \quad (31)$$

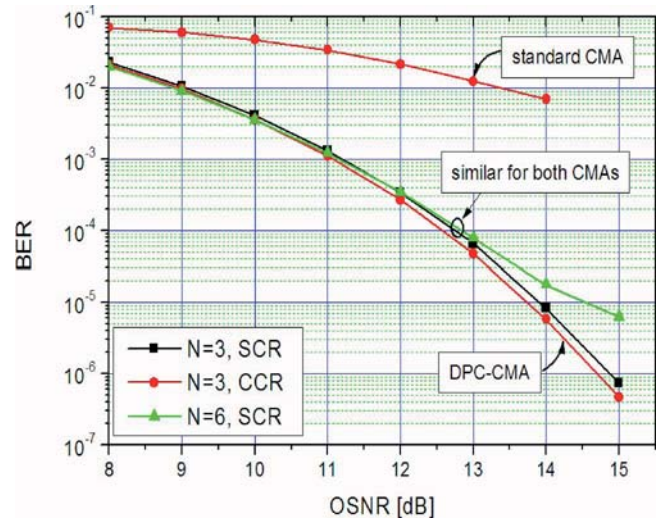


Fig. 3. BER versus OSNR for standard CMA and DPC-CMA with  $g = 2^{-6}$  at different filter widths for common (CCR) and separate (SCR) carrier recoveries. The three lower curves are also approximately valid for ODDA and MDDA, which can always operate with CCR.

As desired, it vanishes for  $\mathbf{M}\mathbf{J} = \mathbf{1}$  and  $\hat{\mathbf{c}} = \mathbf{X}e^{-j\hat{\varphi}}$ . The calculation becomes

$$\mathbf{M} := \mathbf{M} + g\mathbf{T}, \quad \mathbf{T} = \mathbf{E}\mathbf{M} = (\hat{\mathbf{c}} - \mathbf{X}e^{-j\hat{\varphi}})\hat{\mathbf{c}}^+\mathbf{M}. \quad (32)$$

This holds for QPSK as well as for other formats such as 16-QAM. We call this new approach the modified DDA or MDDA, as opposed to the ODDA outlined in [1]. Equation (32) and the auxiliary equations (3) and (24) describe the update of the polarization control matrix coefficients.

## IV. SIMULATION RESULTS

### A. QPSK Simulations

All polarization control algorithms were initially tested in extensive QPSK simulations without added white Gaussian noise and without phase noise. Function, convergence, and DPC (for DPC-CMA and ODDA/MDDA) were verified in all cases.

Next, the polarization control algorithms were compared in Monte Carlo simulations of a polarization-multiplexed QPSK transmission system. Random unitary Jones matrices were set by a random number generator and each data point was based on the simulation of  $(1-15) \times 10^6$  symbols. The sum linewidth times the symbol duration equaled  $\Delta f \cdot T = 10^{-3}$ . Bit error rate (BER) was evaluated only after initial convergence.

In all cases, we have used a carrier recovery according to [13], similar to the one described in [1].

Fig. 3 shows BER versus OSNR for the standard CMA and the DPC-CMA in combination with three different carrier recovery setups. In combination with SCRs, the filter half-widths for the two independent phase estimators are set to  $N = 3$  and  $N = 6$ , i.e., 7 and 13 symbols are used for carrier phase estimation, respectively. These setups are compared with the one with CCR and  $N = 3$ , which uses 14 symbols for phase estimation. In the setups with SCR, the standard CMA and the DPC-CMA have the same efficiency. However, for  $N = 6$  and high OSNR values,

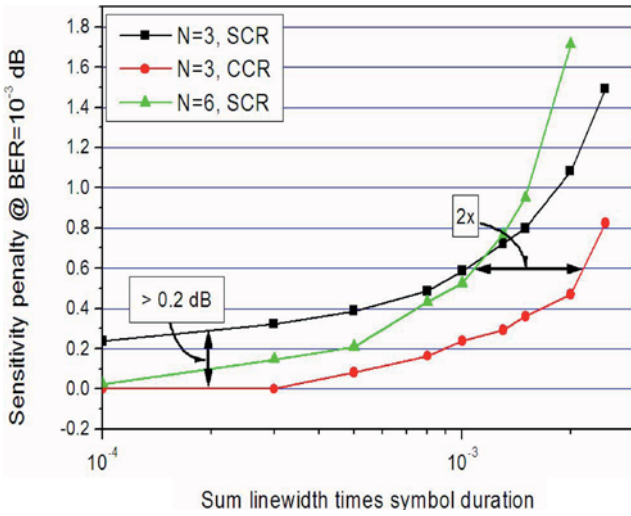


Fig. 4. Sensitivity penalty at  $\text{BER} = 10^{-3}$  for different linewidth times symbol duration products for CCR/SCR. This applies for CMA (with SCR), DPC-CMA (with CCR), and (approximately) for ODDA/MDDA (with CCR), all at small control gains  $g$ .

the sensitivity is affected by phase noise due to the lower filter bandwidth. For  $N = 3$ , there is a general sensitivity penalty of  $\sim 0.2$  dB due to a lower phase estimator efficiency.

With one CCR for both polarization channels, DPC-CMA achieves the same sensitivity as for SCR with  $N = 6$ , but with the same phase noise tolerance as SCR with  $N = 3$ . However, by design, the standard CMA fails with CCR, given that it does not compensate the phase difference between the two polarizations. Thus, the DPC-CMA is required to allow for a CCR. Note that the lower three curves in Fig. 3 also hold (approximately) for ODDA/MDDA with small control gains.

Fig. 4 points out the improved performance due to a CCR enabled by the DPC-CMA. It doubles the phase noise tolerance compared to an SCR that uses the same number of symbols for phase estimation, or it improves the sensitivity by  $> 0.2$  dB compared to an SCR with the same filter halfwidth. The penalty is incurred due to phase noise while polarization recovery is close to perfect. Therefore, the curves also hold approximately when ODDA and MDDA are used, though only CCR makes sense for ODDA/MDDA (whereas SCR is more hardware-intensive).

To give a direct impression, the algorithms were also compared in the time domain for three different gains, with noise. Fig. 5 shows exemplary polarization locking processes for CMA, ODDA, and MDDA. The Jones matrix to be compensated was chosen as

$$\mathbf{J} = \begin{bmatrix} 0.9808 + 0.1951j & 0.4619 - 0.1913j \\ -0.2079 - 0.1389j & 0.7846 - 0.1561j \end{bmatrix} \quad (33)$$

with some polarization-dependent loss (PDL). The compensation matrix was preset as  $\mathbf{M} = \mathbf{1}$ . For all algorithms, the control time constants are on the rough order  $T/g$ , where  $T$  is the symbol duration. From top to bottom in Fig. 5,  $g$  is stepped in factors of 4. The higher the  $g$  is, the noisier is the behavior of the polarization control matrix elements, and the faster is the convergence.

With CMA as a reference, the ODDA performs worse while the MDDA is better, as can be seen from the smaller noise superimposed on the temporal behavior of the matrix element magnitudes.

In order to quantify this, the sensitivity penalty at a  $\text{BER}$  of  $10^{-3}$  was evaluated for all four algorithms (Fig. 6). Reference is the sensitivity of a system with very low polarization control gain ( $g = 0$ ). Linewidth is set to  $\Delta f T = 10^{-4}$ , matrices are unity, and  $\mathbf{M}\mathbf{J} = \mathbf{1}$ . As expected, CMA and DPC-CMA exhibit medium performance. The CMA may be slightly worse than the DPC-CMA due to the need of SCR. A 0.5 dB penalty is reached approximately for  $g \approx 2^{-4}$ . Above that gain, carrier and data recovery soon becomes impossible. This may be due to the nonlinear nature of (4).

The ODDA performs worst, yielding 0.5 dB of penalty already for  $g \approx 2^{-6.4}$ . Best of all is the MDDA, which supports  $g \approx 2^{-3.3}$  at the same penalty.

Thus, for a given penalty of 0.5 dB, CMA/DPC-CMA can control polarization about six times faster than the ODDA, while the MDDA is about 1.6 times faster than CMA/DPC-CMA. The performance gain of MDDA over CMA/DPC-CMA becomes more pronounced if a larger penalty is permissible.

## B. 16-QAM Simulations

All polarization control algorithms were also tested without noise for 4-, 16-, 64-, and 256-QAM, again with their function verified as expected.

The ODDA cannot be recommended for 16- or higher QAM schemes because its gain must be set very low in order to provide adequate averaging. In contrast, the MDDA is unproblematic because the varying signals are correctly taken into account as  $\hat{\mathbf{c}}$  in (32).

Subsequently, we added noise and compared standard CMA [see (4) and (5)], CMA-QAM [see (5), (12), and (13)], and DPC-CMA-QAM [see (8), (9), (12), (13), (17), and (18)] for 16-QAM. For carrier recovery, we took the feedforward algorithm described in [6]. Fig. 7 shows the sensitivity degradation at  $\text{BER} = 10^{-3}$  as a function of control gain  $g$ . Each data point corresponds to 200 000 symbols. A large  $g$  is good for a low small-signal polarization control time constant. The total penalty reaches 2 dB for the standard CMA at  $g \approx 2^{-6.5}$ , while the CMA-QAM can control polarization about three times faster at the same penalty, with  $g = 2^{-5}$ . For both, the two carrier recoveries processed 19 symbols in parallel. The DPC-CMA-QAM with one CCR for both polarizations processes only nine temporal samples, and therefore, either increases sensitivity by  $\sim 0.5$  dB at the chosen sum linewidth times symbol duration product of  $\Delta f T = 2 \times 10^{-4}$ , or maintains the same sensitivity at a doubled  $\Delta f T = 4 \times 10^{-4}$ . Other than in [7], the 0 dB reference of Fig. 7 is not the theoretical sensitivity but the (slightly worse) sensitivity that is achieved with  $\Delta f T = 0$ ,  $g = 0$ , and  $\mathbf{M}\mathbf{J} = \mathbf{1}$ .

For the scenario  $\Delta f T = 0$  and  $\mathbf{M}\mathbf{J} = \mathbf{1}$ , reference  $g = 0$ , three CMAs, ODDA, and MDDA are compared in Fig. 8. Penalty traces for CMA-QAM and DPC-CMA-QAM are fairly identical, as  $\Delta f T = 0$ . At 0.5 dB penalty, the MDDA is  $\sim 15$  times

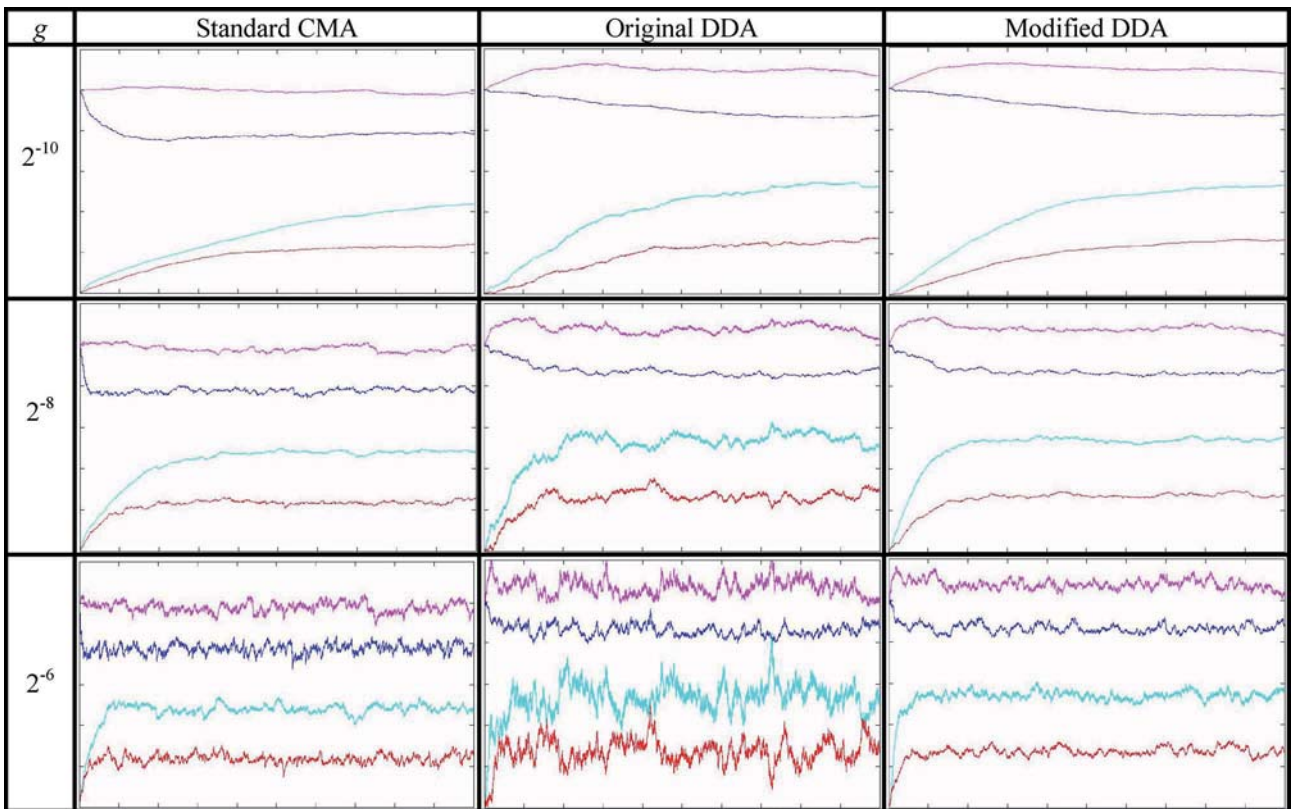


Fig. 5. Example for the start-up development of the element magnitudes of matrix  $M = [m_{ij}]$ . Horizontal axis: 0–5000 symbol durations. Vertical axis: 0–1.2. Traces (from to bottom):  $|m_{22}|$ ,  $|m_{11}|$ ,  $|m_{12}|$ ,  $|m_{21}|$ .

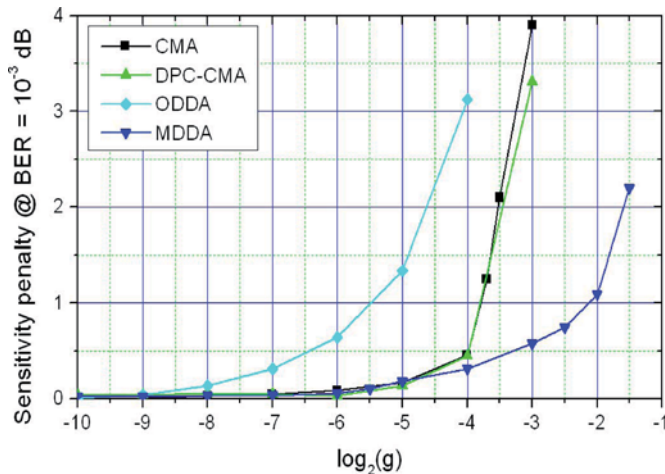


Fig. 6. Influence of polarization control gain  $g$  on QPSK receiver sensitivity. DPC-CMA, ODDA, and MDDA are with common, CMA with SCRs.

faster than the standard CMA and  $\sim 4$  times faster than the DPC-CMA-QAM.

V. HARDWARE EFFORT COMPARISON

We compare the hardware implementation effort by the number of multiplications to be carried out.

The multiplication  $\mathbf{MR}$  means four complex multiply-and-accumulate operations (CMAC) for each of the algorithms. One

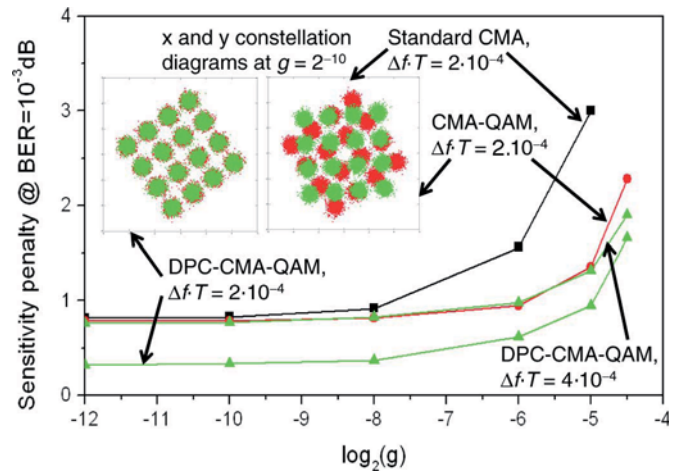


Fig. 7. Sensitivity of various CMAs applied to polarization-multiplexed 16-QAM signals versus control gain  $g$ . Unlike the others, DPC-CMA-QAM nullifies the phase difference between the  $x$  and  $y$  constellation diagrams, and therefore, tolerates one CCR for both polarizations.

CMAC contains four real multiplications. For QPSK, (25) and (26) contain only two CMAC each, since the multiplication by  $\hat{c}^+$  can be trivialized into additions/subtractions/quadrant changes. The multiplication by  $\mathbf{M}$  in the alternative matrix updating equations (29) or (32) needs another four CMAC, yielding a total of 12 CMAC for ODDA and MDDA.

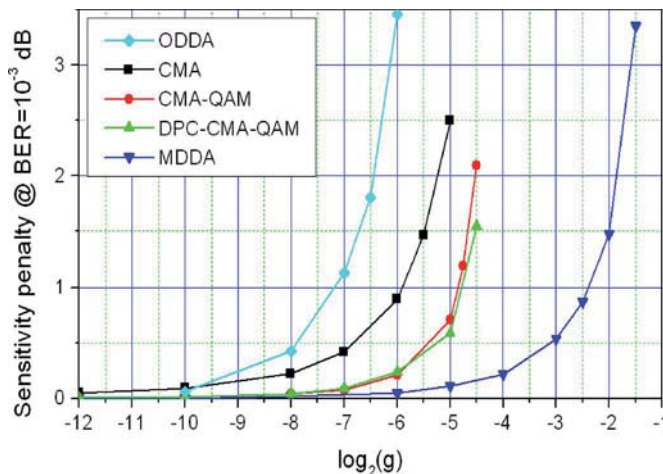


Fig. 8. Influence of polarization control gain  $g$  on 16-QAM receiver sensitivity for  $\Delta fT = 0$  and  $\mathbf{M}\mathbf{J} = \mathbf{1}$ . MDDA outperforms all other algorithms.

Equation (4) can be cast into eight CMAC, which also results in the total number of 12 CMAC as for the standard CMA. In order to avoid doubled carrier recovery effort, DPC is recommended. The DPC equation (9) requires the multiplication of  $\mathbf{M}$  by a scalar. This amounts to eight real multiplications, equivalent to two extra CMACs for DPC-CMA.

The use of 16-QAM instead of QPSK causes moderate extra effort for MDDA and CMA-QAM, due to the fact that the larger quantization of recovered symbols must be taken into account. But for 16-QAM, the carrier recovery is relatively complicated. In order to avoid doubled effort due to SCRs, it is even more advised to supplement the CMA-QAM by DPC. This needs quite some hardware effort.

Summarizing the hardware efforts, ODDA, MDDA, and the CMAs are of similar complexity, but for 16-QAM, the recommended DPC effort makes the CMA-QAM less attractive than MDDA.

Performance-wise, the MDDA is better than the CMA, which, in turn, is better than ODDA.

Altogether, usage of the MDDA is recommended.

## VI. CONCLUSION

In a polarization-multiplexed coherent QPSK transmission system, the standard CMA can be used only with SCRs. But the DPC-CMA compensates the phase difference between the polarization channels. This allows to work with a simpler CCR in the receiver, and thus, to improve phase noise tolerance or sensitivity. Both CMAs tolerate high control gains up to  $g \approx 2^{-4}$ . When extended to QAM with additional DPC, the resulting DPC-CMA-QAM permits QAM transmission with doubled laser linewidth tolerance, due to the use of a CCR for both polarizations. Polarization control speed is tripled.

Decision-directed polarization recovery in its original fashion (ODDA) is about six times slower than CMA. But in a modified version of the MDDA, it is about 1.6 times faster than the CMA and tolerates QAM modulation formats, with higher speed gain.

Due to its superior performance and moderate implementation effort, we recommend using the MDDA.

## REFERENCES

- [1] R. Noé, "PLL-free synchronous QPSK polarization multiplex/diversity receiver concept with digital I&Q baseband processing," *IEEE Photon. Technol. Lett.*, vol. 17, no. 4, pp. 887–889, Apr. 2005.
- [2] T. Pfau, R. Peveling, H. Porte, Y. Achiam, S. Hoffmann, S. K. Ibrahim, O. Adamczyk, S. Bhandare, D. Sandel, M. Porrmann, and R. Noé, "Coherent digital polarization diversity receiver for real-time polarization-multiplexed QPSK transmission at 2.8 Gbit/s," *IEEE Photon. Technol. Lett.*, vol. 19, no. 24, pp. 1988–1990, Dec. 2007.
- [3] D. Godard, "Self-recovering equalization and carrier tracking in two-dimensional data communication systems," *IEEE Trans. Commun. Technol.*, vol. COM-28, no. 11, pp. 1867–1875, Nov. 1980.
- [4] K. Kikuchi, "Polarization-demultiplexing algorithm in the digital coherent receiver," in *Proc. IEEE/LEOS Summer Topical Meetings*, Jul. 21–23, 2008, pp. 101–102, Paper MC2.2.
- [5] M. El-Darawy, T. Pfau, S. Hoffmann, and R. Noé, "Differential phase compensated constant modulus algorithm for phase noise tolerant coherent optical transmission," in *Proc. IEEE-LEOS 2009*, San Diego, CA, Jul. 20–22, pp. 95–96, Paper TuC3.3.
- [6] T. Pfau, S. Hoffmann, and R. Noé, "Hardware-efficient coherent digital receiver concept with feedforward carrier recovery for M-QAM constellations," *J. Lightw. Technol.*, vol. 27, no. 8, pp. 989–999, Apr. 2009.
- [7] R. Noé, T. Pfau, and M. El-Darawy, "QAM adaptation of constant-modulus algorithm and differential phase compensation for polarization demultiplex in coherent receiver," presented at the Eur. Conf. Opt. Commun. (ECOC 2009), Vienna, Austria, Sep. 20–24, Paper We7.3.3.
- [8] X. Zhou, J. Yu, and P. Magill, "Cascaded two-modulus algorithm for blind polarization demultiplexing of 114-Gb/s PDM-8-QAM optical signals," in *Proc. OFC 2009, OWG3*, pp. 1–3.
- [9] H. Louchet, K. Kuzmin, and A. Richter, "Improved DSP algorithms for 16-QAM transmission," in *Proc. ECOC 2008*, pp. 1–2, Paper TU.1.E.6.
- [10] M. J. Ready and R. P. Gooch, "Blind equalization based on radius directed adaptation," in *Proc. 1990 Int. Conf. Acoust., Speech, Signal Process. (ICASSP)*, Apr. 3–6, vol. 3, pp. 1699–1702.
- [11] M. El-Darawy, T. Pfau, S. Hoffmann, R. Peveling, C. Wördehoff, B. Koch, M. Porrmann, O. Adamczyk, and R. Noé, "Fast adaptive polarization and PDL tracking in a real-time FPGA-based coherent PolDM-QPSK receiver," *IEEE Photon. Technol. Lett.*, vol. 20, no. 21, pp. 1796–1798, Nov. 2008.
- [12] M. Kuschnerov, D. van den Borne, K. Piyawanno, F. N. Hauske, C. R. S. Fludger, T. Duthel, T. Wuth, J. C. Geyer, C. Schullien, B. Spinnler, E.-D. Schmidt, and B. Lankl, "Joint-polarization carrier phase estimation for XPM-limited coherent polarization-multiplexed QPSK transmission with OOK-neighbors," presented at the Eur. Conf. Opt. Commun. (ECOC), Brussels, Belgium, Sep. 21–25, 2008, Paper Mo4.D.2.
- [13] S. Hoffmann, R. Peveling, T. Pfau, O. Adamczyk, R. Eickhoff, and R. Noé, "Multiplier-free real-time phase tracking for coherent QPSK receivers," *IEEE Photon. Technol. Lett.*, vol. 21, no. 3, pp. 137–139, Feb. 2009.



**Reinhold Noé** (M'93–SM'09) was born in Darmstadt, Germany, in 1960. He received the Dipl.-Ing. and Dr.-Ing. degrees in electrical engineering from the Technische Universität München, Munich, Germany, in 1984 and 1987, respectively.

He realized the first endless polarization control systems. He was a Postdoctoral Fellow with Bellcore, Red Bank, NJ, where he worked on coherent optical systems. In 1988, he joined Siemens Research Laboratories, Munich. In 1992, he implemented the first synchronous optical phase-shift keying (PSK) transmission with normal distributed feedback (DFB) lasers. Since 1992, he has been the Chair of the Optical Communication and High-Frequency Engineering, University of Paderborn, Paderborn, Germany. His current research interests include high-speed endless optical polarization control and real-time synchronous QPSK transmission. He has authored or coauthored more than 200 journal and conference publications.

Dr. Noé is a member of the Verband der Elektrotechnik Elektronik Informationstechnik e.V. (VDE).



**Timo Pfau** (M'08) was born in Stuttgart, Germany, in 1979. He received the Dipl.-Ing. degree in electrical engineering and information technology from the University of Stuttgart, Stuttgart, in 2004, and the Dr.-Ing. degree (with highest honors) in electrical engineering from the University of Paderborn, Paderborn, Germany, in 2009.

After graduation, he was granted a scholarship from the International Graduate School "Dynamic Intelligent Systems," University of Paderborn. Since June 2009, he has been a member of the Technical Staff at Bell Laboratories, Alcatel-Lucent, Murray Hill, NJ. His current research interests include algorithm development for coherent optical receivers with digital signal processing and real-time implementation of coherent optical transmission systems using advanced modulation formats.

Dr. Pfau is a reviewer for *IEEE Photonics Technology Letters* and the *IEEE Journal of Lightwave Technology*. He is a member of the Verband der Elektrotechnik Elektronik Informationstechnik e.V. (VDE).



**Sebastian Hoffmann** (M'09) was born in Bielefeld, Germany, in 1969. He received the Dipl.-Ing., Dipl.-Wirt.-Ing., and Dr.-Ing. degrees from the University of Paderborn, Paderborn, Germany, in 1997, 2000, and 2008, respectively.

From 1988 to 1992, he was on vocational training as a Power Electronics Technician at Miele & Cie. KG, Bielefeld, Germany. Then, he studied electrical engineering in Paderborn, Germany, and Waterloo, ON, Canada. After graduation, he was a Postdoctoral Researcher. He is currently with the Optical Communication and High-Frequency Engineering, University of Paderborn. He has contributed to various projects, including microelectronics, high-frequency engineering, and optical communication.

Dr. Hoffmann is a reviewer for the *IEEE PHOTONICS TECHNOLOGY LETTERS* and the *IEEE Journal of Lightwave Technology*.



**Mohamed El-Darawy** (S'09) was born in Cairo, Egypt, in 1974. He received the Master's degree in optical communication from the Physics Department, Faculty of Science, Ain Shams University, Cairo, in 2001. He is currently working toward the Ph.D. degree at the University of Paderborn, Paderborn, Germany.

He was a Teaching Assistant at Ain Shams University. After graduation, he was granted a scholarship from the Ministry of Higher Education in Egypt to study the Ph.D. degree. His current research interests include algorithm development for coherent optical receivers with digital signal processing and real-time implementation of coherent optical transmission systems using advanced modulation formats.